IJMMM International Journal of Minerals, Metallurgy and Materials 矿物冶金与材料学报（英文版）

Alkyl dimethyl betaine activates the low-temperature collection capacity of sodium oleate for scheelite

Xu Wang, Zhengquan Zhang, Yanfang Cui, Wei Li, Congren Yang, Hao Song, Wenqing Qin, and Fen Jiao

Cite this article as:
Xu Wang, Zhengquan Zhang, Yanfang Cui, Wei Li, Congren Yang, Hao Song, Wenqing Qin, and Fen Jiao, Alkyl dimethyl betaine activates the low-temperature collection capacity of sodium oleate for scheelite, *Int. J. Miner. Metall. Mater.*, 31(2024), No. 1, pp. 71-80. https://doi.org/10.1007/s12613-023-2718-2

View the article online at SpringerLink or IJMMM Webpage.

INTERNATIONAL JOURNAL OF
Minerals, Metallurgy and Materials

Volume 31, Number 1, January 2024
Page 71

Research Article https://doi.org/10.1007/s12613-023-2718-2

Alkyl dimethyl betaine activates the low-temperature collection capacity of sodium oleate for scheelite

Xu Wang[1,2,4], *Zhengquan Zhang*[1,2], *Yanfang Cui*[1,2], *Wei Li*[1,2], *Congren Yang*[1,2], *Hao Song*[3,4], *Wenqing Qin*[1,2)✉], *and Fen Jiao*[1,2)✉]

1) School of Minerals Processing and Bioengineering, Central South University, Changsha 410083, China
2) Key Laboratory of Hunan Province for Clean and Efficient Utilization of Strategic Calcium-containing Mineral Resources, Central South University, Changsha 410083, China
3) College of Engineering, Drexel University, Philadelphia, PA 19102, USA
4) Luoyang Zhenbei Industry and Trade Co., Ltd., Luoyang 47100, China
(Received: 31 May 2023; revised: 23 July 2023; accepted: 7 August 2023)

Abstract: The impact of alkyl dimethyl betaine (ADB) on the collection capacity of sodium oleate (NaOl) at low temperatures was evaluated using flotation tests at various scales. The low-temperature synergistic mechanism of ADB and NaOl was explored by infrared spectroscopy, X-ray photoelectron spectroscopy, surface tension measurement, foam performance test, and flotation reagent size measurement. The flotation tests revealed that the collector mixed with octadecyl dimethyl betaine (ODB) and NaOl in a mass ratio of 4:96 exhibited the highest collection capacity. The combined collector could increase the scheelite recovery by 3.48% at low temperatures of 8–12°C. This is particularly relevant in the Luanchuan area, which has the largest scheelite concentrate output in China. The results confirmed that ODB enhanced the collection capability of NaOl by improving the dispersion and foaming performance. Betaine can be introduced as an additive to NaOl to improve the recovery of scheelite at low temperatures.

Keywords: scheelite; betaine; low temperature; synergistic effect; dispersion; foamability

1. Introduction

Fatty acids and their soaps are commonly used as collectors for non-sulfide minerals such as scheelite, fluorite, apatite, bauxite, and hematite [1–5]. The traditional fatty acid collectors (FAC) include oleic acid, sodium oleate (NaOl), tall oil, and oxidized paraffin soap [6–7]. Related studies have confirmed that FACs are adsorbed on the mineral surface through the chemical interactions between the FAC carboxylic acids and mineral surface cations, making the mineral surface hydrophobic. FACs not only have good collection capacity but also foaming ability. However, the water solubility and dispersibility of FACs are poor, particularly at low temperatures. As a result, low temperatures can deteriorate the collection capacity of FACs and reduce the recovery efficiency of the target minerals [8].

Modification and reagent combination are the two important approaches to improving the collection capacity of FAC at low temperatures. The term modification refers to the introduction of new polar groups into the FAC molecule, involving complex chemical reactions such as halogenation, sulfation, etherification, and hydroxylation of fatty acids. However, complex chemical processes usually imply environmental pollution and high costs. In contrast, the solution for reagent combination has low cost, simple operation, and less risk of environmental pollution, making this process suitable for industrial production. Reagent combination can improve the recovery of target minerals by co-adsorption, increasing the solubility and dispersion of reagents, or changing the properties of the flotation foam [9–16]. Related studies have indicated that fatty alcohols and oleic acid can co-adsorb and form complexes on the mineral surface. These complexes replace the oleate dimer on the mineral surface, which enhances the hydrophobicity of the mineral surface and significantly improves the recovery of fluorapatite and calcite [17]. The synergistic effect between the nonionic surfactants polyethoxyalkyl ether and NaOl can effectively reduce the critical micelle concentration (CMC) as well as improve the foamability and foam stability of the NaOl solution [18–19]. This finding has been applied to the low-temperature flotation of scheelite [20]. Tween 80 can enhance the adsorption density of NaOl on the surface of magnesite by improving its solubility and dispersibility, thereby increasing the recovery of magnesite [21].

Alkyl dimethyl betaine (ADB) is an amphoteric surfactant. As shown in Fig. S1, ADB has a quaternary ammonium

✉ Corresponding authors: Wenqing Qin E-mail:qinwenqing369@126.com; Fen Jiao E-mail: jfen0601@126.com

internal salt structure, also known as an ammonium structure. Its anionic group is a carboxyl group, and the carbon number of the hydrocarbon chain R is 12–18. Given its amphoteric nature, ADB not only has good dispersion, emulsification, and foaming properties but also has a wide range of pH adaptability [22–23]. Hence, ADB has been widely applied in various fields [24–26]. However, relatively few reports were found on the application of ADB in flotation.

The deterioration of the collection capacity of FAC at low temperatures in winter is a common phenomenon in scheelite plants in northern China [27], which can cause a sharp increase in the production cost and tailings reservoir load, as well as a large loss of tungsten resources. If ADB is applied to the flotation recovery of scheelite in a low-temperature environment, it can ameliorate the adverse effects of a complex pulp environment and greatly improve the utilization efficiency of scheelite resources because of its amphoteric structure. This was the motivation for studying the synergistic effect of ADB of different chain lengths on the NaOl–scheelite flotation system. The effect of the combined collector was investigated by micro-flotation tests and actual ore flotation tests. The synergistic mechanism of ADB was revealed by Fourier transform infrared spectroscopy (FTIR), X-ray photoelectron spectroscopy (XPS), surface tension measurement, foam performance testing, and flotation reagent size measurement. The result of this study can help address low scheelite recovery and low FAC activity at low temperatures, which is of great significance to scheelite resource recovery technology.

2. Experimental

2.1. Mineral samples and reagents

2.1.1. Single minerals

Scheelite crystals were obtained from Huadong Tangtang Handicraft Factory, Guangdong, China. Bulk samples were manually crushed, and the impurities were removed before grinding and sieving. Powder samples with a particle size of −0.074+0.037 mm were subjected to micro-flotation after homogenization. The remaining samples with a particle size of −0.037 mm were further characterized by X-ray fluorescence (XRF) (Table S1), X-ray diffraction (XRD) (Fig. 1), etc. The XRF analysis results indicated that the purity of scheelite was 96.23%, based on the conversion of the WO_3 grade of 77.56%. Characteristic peaks of other minerals were not observed in the XRD spectra, which demonstrates that the purity of scheelite was sufficient for micro-flotation tests.

2.1.2. Characterization of the actual ore

Typical samples of the actual ore and molybdenum tailings were obtained from China Molybdenum Co., Ltd. (CMOC) [28]. As shown in Table S2, the Mo and W content in the actual ore was 0.135wt% and 0.052wt%, respectively. The results of the mineral liberation analyzer shown in Table S3 indicated that molybdenum primarily exists in the form of pyromorphite and that tungsten exists in the form of scheelite. Gangue minerals were mainly comprised of calcareous gangue and siliceous gangue. The recovery of molybdenite is typically followed by the recovery of scheelite during industrial production. Fig. 2 presents the WO_3 distribution in molybdenum tailings, with most of the WO_3 distributed in particles with a size of −0.038 mm.

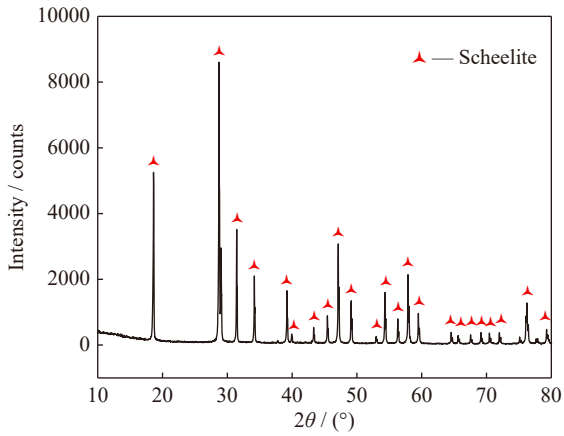

Fig. 1. XRD analysis spectra of the scheelite sample.

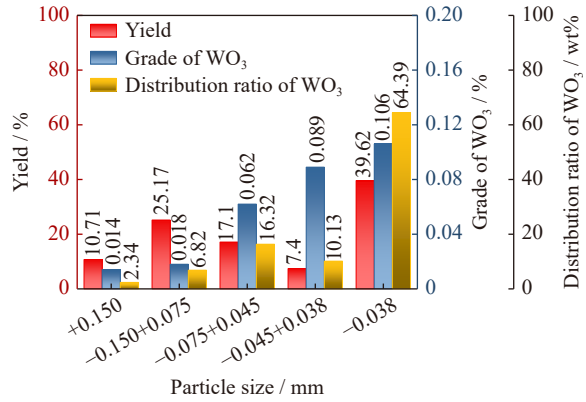

Fig. 2. Distribution of the particle size and WO_3 content in molybdenite flotation tailings.

2.1.3. Reagents

The pH regulators sodium hydroxide (NaOH) and sulfuric acid (H_2SO_4) used in the micro-flotation test were produced by Tianjin Damao Chemical Reagent Factory. The NaOl collector was obtained from Luoyang Zhenbei Industry and Trade Co., Ltd., with an effective content of not less than 90wt%. Betaine surfactants were purchased from Shanghai Shengxuan Bio-chemical Co., Ltd., including dodecyl dimethyl betaine (DDB), tetradecyl dimethyl betaine (TDB), and octadecyl dimethyl betaine (ODB). The resistivity of the deionized water used in the test was greater than 18.0 MΩ·cm.

2.2. Flotation tests

2.2.1. Micro-flotation tests

Micro-flotation tests were performed on an XFG flotation machine (Jilin Exploration Machinery Plant, Changchun, China). The deionized water and single mineral samples used in the low-temperature flotation tests were frozen, and ice packs were tied outside the flotation cell. The flotation temperature was maintained at 10–12°C. As shown in Fig. S2, 2.0 g of a single mineral and 35 mL of deionized water were

placed together in a 40 mL flotation cell. After stirring for 1 min, the regulator and collector were added sequentially. The stirring time for each flotation reagent and flotation time was 3 min. The concentrate and tailings were filtered, dried, and weighed separately to calculate the scheelite recovery. The data presented are the average of three replicate tests under the same conditions. The standard deviation of the results was calculated and is indicated by error bars.

2.2.2. Batch flotation tests

Batch flotation tests of the actual ore were performed using an XFD flotation machine (Jilin Exploration Machinery Plant, Changchun, China). The batch flotation temperature was maintained at 10–12°C, just like the micro-flotation test. The desired dosages of flotation reagents were added successively to the flotation cell. All concentrates and tailings obtained from the batch flotation tests were filtered, dried, weighed, and assayed to calculate the scheelite recovery. Each test was repeated three times to ensure accuracy.

2.2.3. Industrial tests

The industrial test was conducted in the roughing workshop of a scheelite plant in Luanchuan. Sodium carbonate, sodium silicate, and NaOl were used as the pH regulator, inhibitor, and collector, respectively, in the roughing stage [29]. The traditional "Petrov process" was adopted for the cleaning stage [30]. The roughing stage was conducted at room temperature, while the cleaning stage required heating of the pulp to above 90°C. As shown in Fig. S3, the series I and II of the roughing workshop, having the same feeding, configuration and processing capability, were deployed to compare the performance of the collectors. During industrial commissioning, the indices of each series were summarized, and the collector performance evaluated in detail.

2.3. FTIR spectra

The interaction between collectors and scheelite was characterized by an FTIR (IRAffinity-1, Shimadzu Corporation, Kyoto, Japan) in the KBr diffuse reflection mode [28,31]. The samples to be tested were prepared as follows: 30 mg of the mineral scheelite was dispersed in 100 mL of deionized water, and the pulp temperature was kept at 10°C. Then, the pulp pH was adjusted to 9.5, and a certain concentration of the flotation reagent was added. After stirring the pulp with a magnetic stirrer for 30 min, the sample was filtered and washed three times with deionized water of the same pH. The sample was dried in a constant-temperature vacuum oven at 40°C.

2.4. XPS measurement

XPS characterization was performed using a Thermo Scientific K_α X-ray photoelectron spectrometer (Thermo Fisher Scientific, USA), using an Al K_α ($h\nu$ = 1486.6 eV) X-ray source, a beam spot size of 400 μm, working voltage of 12 kV, filament current of 6 mA, with the analysis chamber at a vacuum better than 5.0×10^{-7} mBar, and step sizes for the survey spectrum and fine spectrum of 1.0 and 0.05 eV, respectively. The sample treatment process was consistent with the micro-flotation test. The measurement results were processed using Avantage. The energy standard for charge correction was C 1s = 284.80 eV.

2.5. Surface tension measurement

The CMC is an important parameter to measure the activity of surfactants and represents the minimum concentration at which large amounts of micelle can be formed in a surfactant solution. The smaller the CMC, the more efficient the activation of the surfactant, resulting in a lower concentration required for solubilization, emulsification, and foaming [32–35]. After the concentration exceeded the CMC, there was very little change in the surface tension of the surfactant, which can be used to determine the CMC of different collector solutions. Surface tension measurement was performed using a fully automatic surface/interface tension meter (BZY-2, Shanghai HengPing Instrument and Meter Factory) at a low temperature of 10°C [36].

2.6. Foam performance testing and evaluation

The foamability and the foam stability of the collector are critical to the recovery of scheelite. The foam properties of the collector were measured using the airflow method [37]. As shown in Fig. S4, the airflow measuring device is a graduated cylindrical glass tube with a capillary tube at the bottom. The collector solution was added using a long-necked funnel to ensure that the glass tube walls remained dry. Then, the glass was inflated at a rate of 80 mL/min for 2 min, and the foam volume at the end of the inflation was used to characterize the foaming performance of the collector. Finally, the time required for the foam to decay to half its original height was used to characterize the stability of the foam. The diameter and height of the foam tube were 40 and 350 mm, respectively. In addition, the hole diameter of the sand core under the foam tube was 5 mm.

2.7. Flotation reagent size measurement

A nanoparticle-size and zeta potential analyzer (Malvern-Zetasize Nano-90) was used to measure the particle-size distribution in different collector solutions, and the dispersion of the reagent was visually characterized at the same concentration. The test range of the analyzer was 0.4–10.0 μm. The measurements were repeated three times for each condition, and the results were presented as the averages.

3. Results and discussion

3.1. Flotation test results

3.1.1. Micro-flotation test results

(1) Effect of the pulp temperature on the collection capacity of NaOl. Based on previous studies, pulp pH was fixed at a suitable value of 9.5 ± 0.1 for scheelite flotation [28]. As shown in Fig. 3, scheelite recovery reaches a high value of 92% when the concentration of NaOl is 20 mg/L at room temperature (28–30°C). However, the maximum recovery of scheelite at a NaOl concentration of 60 mg/L at a low tem-

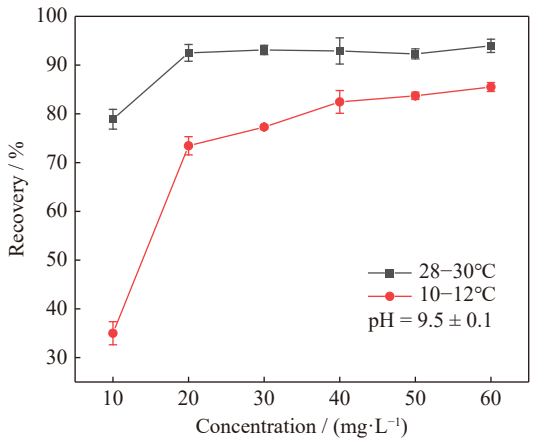

Fig. 3. Effect of pulp temperature on the collection capacity of NaOl.

perature of 10–12°C is only 85%. The results indicated that the low temperature adversely affects the dispersibility and solubility of NaOl, thereby increasing the consumption of the collector and decreasing scheelite recovery.

(2) Effect of ADB on the collection capacity of NaOl at low temperatures. The effect of ADB with different chain lengths on the collection capacity of NaOl at different addition mass ratios was investigated in detail. The pulp pH was fixed at 9.5 ± 0.1, and the pulp temperature was maintained at 10–13°C. As shown in Fig. 4, the addition of ADB significantly optimized the collection capacity of NaOl for scheelite at low temperatures, and more abundant foam could be observed during flotation. The optimal addition ratio of DDB was found to be 16wt%, with the scheelite recovery reaching up to about 89% at a collector concentration of 30 mg/L. The preferred addition ratio of TDB is 4wt%, at which the maximum scheelite recovery is about 87% at a collector concentration of 30 mg/L. The optimal addition ratio of ODB is also 4wt%, with the scheelite recovery reaching an ideal value of about 91% at a collector concentration of 30 mg/L. The results indicated that ODB significantly improves the capacity of NaOl to collect scheelite at low temperatures. The scheelite recovery can be increased by about 6% at the optimum ratio of ODB compared with using NaOl alone. However, scheelite could not be collected directly using only ADB. Therefore, ADB can only activate the collection of NaOl scheelite by optimizing the dispersion and foaming ability at low temperatures.

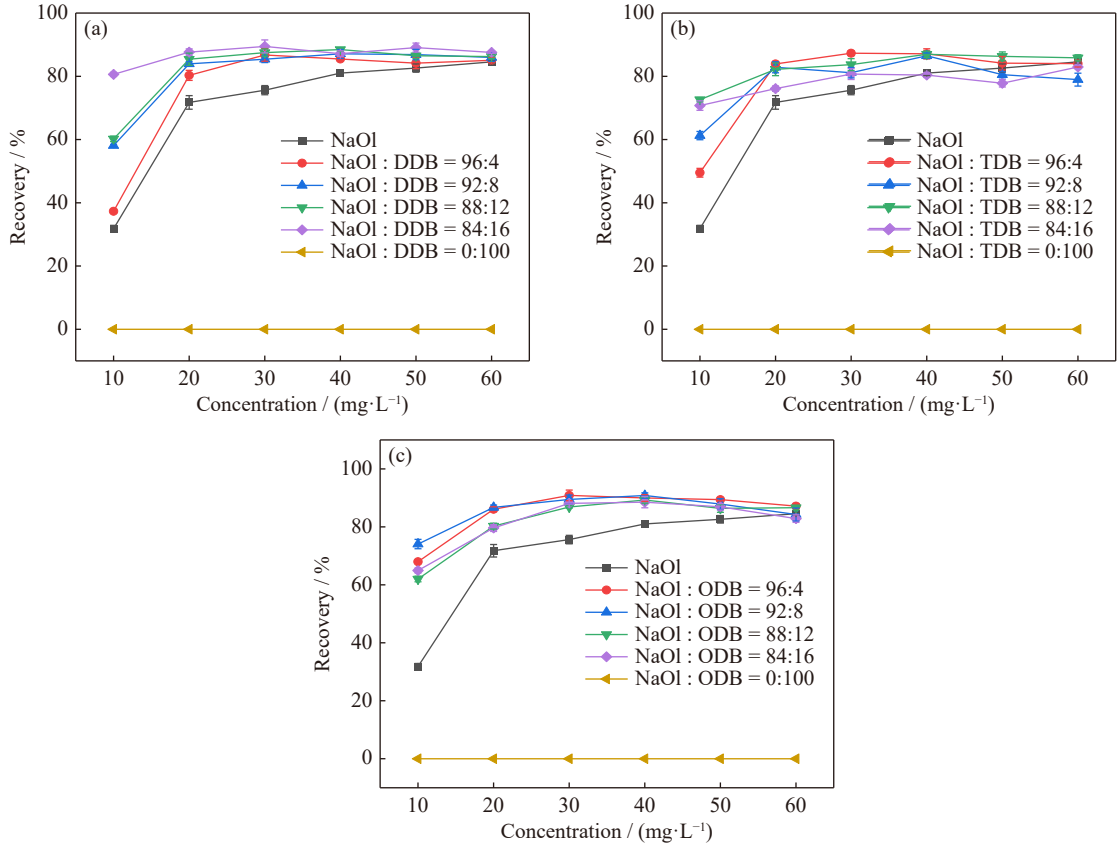

Fig. 4. Effect of ADB on the collection capacity of NaOl: (a) DDB; (b) TDB; (c) ODB.

3.1.2. Batch flotation test results

The synergistic effect of ADB on the collection capacity of NaOl at low temperatures was further evaluated by testing the actual ore at a laboratory scale. The concentration of the flotation reagents for scheelite was controlled at the optimal level and at low temperatures: 1800 g/t of sodium carbonate, 200 g/t of water glass, and 360 g/t of the collector. As shown in Fig. 5, ODB exhibits a more pronounced synergistic effect than DDB and TDB when the addition ratio is 4wt%. As compared to NaOl alone, the mixture of NaOl and ODB can increase the scheelite recovery from 62.37% to 69.89%, and the WO_3 grade of the rough concentrate reduces from

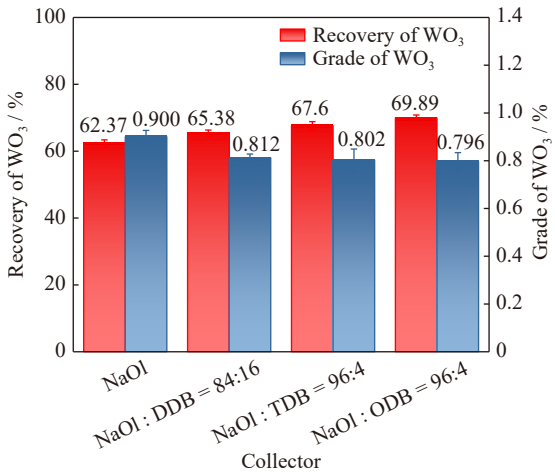

Fig. 5. Results of the batch flotation test.

0.900% to 0.796%.

3.1.3. Industrial test results

Industrial tests were conducted from 28 December 2019 to 3 January 2020 in three 8-h shifts per day, during which the slurry temperature ranged from 8 to 12°C. The combined collector was prepared with NaOl and ODB in a mass ratio of 96:4. As shown in Fig. 6, scheelite recovery of series I with the combined collector was higher than that of series II with NaOl in most shifts. As compared with the index before industrial commissioning, the cumulative recovery of series I and series II during industrial commissioning increased by 7.16% and 3.68%, respectively. Therefore, excluding feeding quality fluctuations and system errors, the application of the combined collector was able to increase the scheelite recovery by 3.48% at low temperatures. Moreover, a flotation column that could reduce gangue entrainment was used in industrial production. Hence, the WO_3 grade of the rough concentrate obtained by the combined collector did not decrease significantly. Meanwhile, the dosage of the combined collector was 28 g/t lower than that of NaOl. The industrial test results confirmed that ODB can improve the collection capacity of NaOl for scheelite at low temperatures.

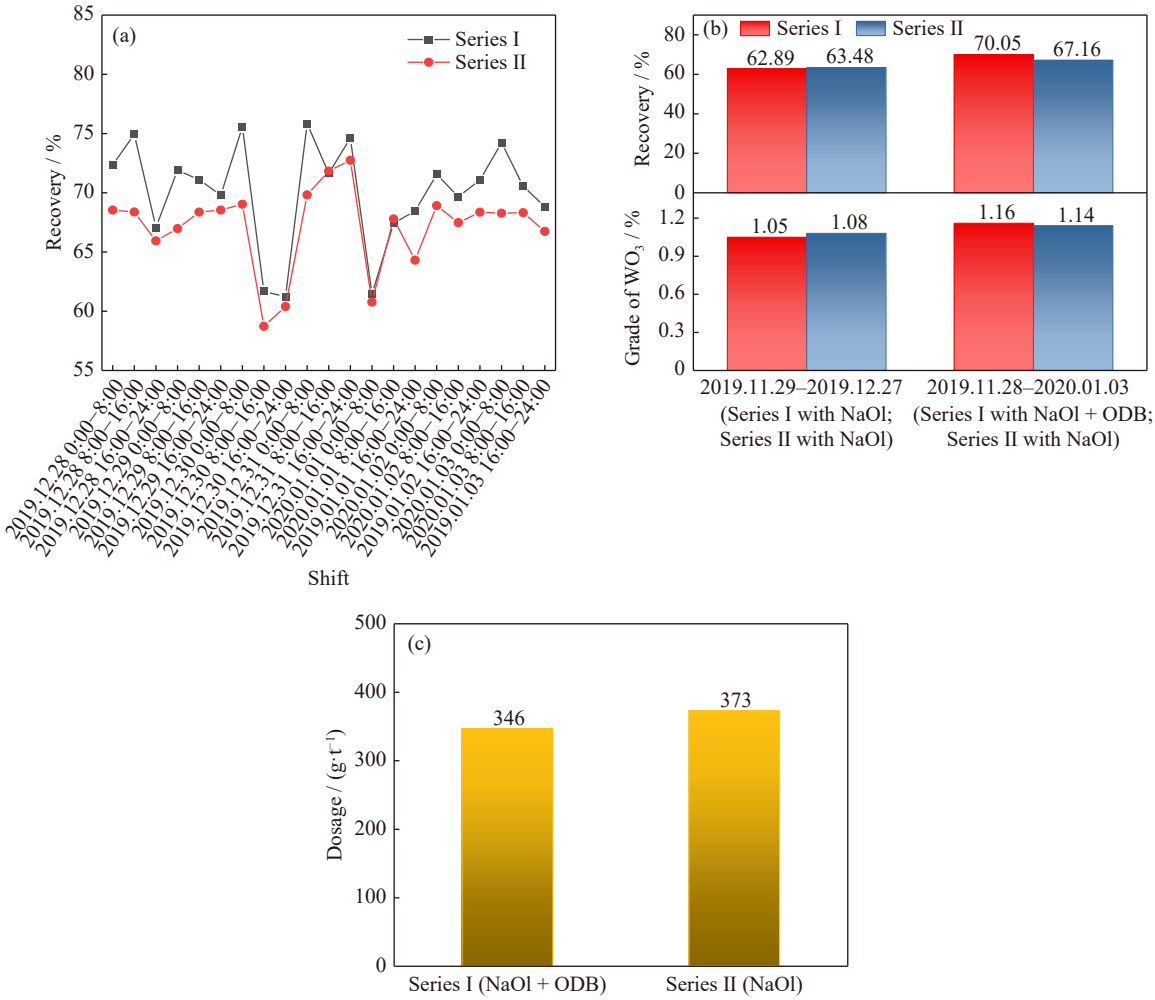

Fig. 6. Results of the industrial test: (a) scheelite recovery of each shift, (b) cumulative recovery before and after the industrial test, and (c) average dosage of collectors.

3.2. FTIR spectral analysis results

The infrared spectrum was used to delve into whether NaOl and ODB co-adsorbed on the scheelite surface. The FITR spectrum of NaOl (Fig. 7(a)) shows bands present at 1461.78 and 1552.42 cm^{-1}, corresponding to the stretching vibration of carboxyl (–COOH). The bands at 2925.48 and 2854.13

cm^{-1} can be attributed to the stretching vibration of methylene ($–CH_2–$) or methyl ($–CH_3$) groups. The bands of $–CH_2–$ and $–CH_3$ in ODB occur at 2924.74 and 2854.54 cm^{-1} [28,38–40]. In addition, the bands at 1630.63 and 1485.85 cm^{-1} are due to the skeleton vibration of nitrogen (N) in ODB. The stretching vibration band of C–N in ODB appears at 1333.39 cm^{-1}. The stretching vibration bands of –COOH can be observed at 1398.72 and 1073.48 cm^{-1} [23,41–43]. The ammonium group is the main characteristic group that distinguishes ODB from NaOl.

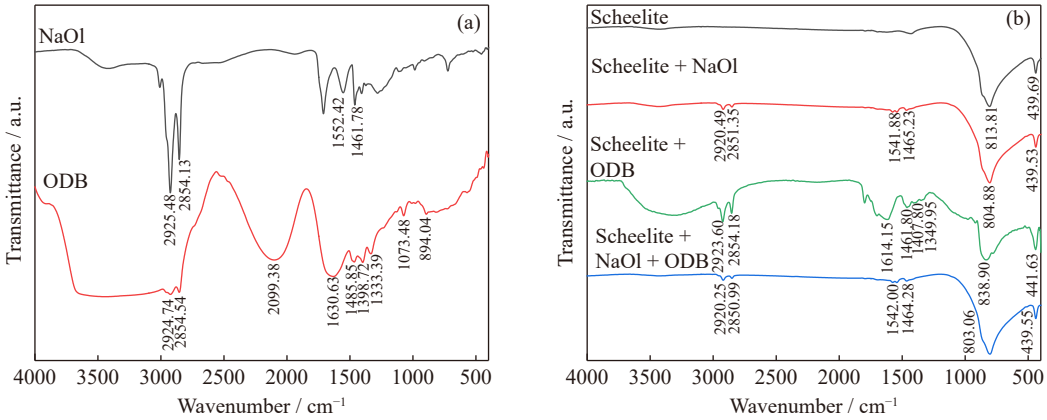

Fig. 7. FTIR spectra of reagents and minerals: (a) NaOl and ODB; (b) scheelite reacted with different collectors.

The infrared spectra of scheelite with different collectors are shown in Fig. 7(b). The infrared spectrum of bare scheelite shows bands corresponding to W–O stretching and bending vibrations inherent in scheelite at 813.81 and 439.69 cm^{-1}, respectively. After being treated with NaOl, new bands emerged at 2920.49 and 2851.35 cm^{-1}, corresponding to the stretching vibrations of $–CH_2–$ and $–CH_3$. The new bands at 1541.88 and 1465.23 cm^{-1} were assigned to –COOH. The results indicated that NaOl was adsorbed on the scheelite surface. In the presence of ODB alone, the characteristic bands of $–CH_2–$, $–CH_3$, and –COOH can be observed at 2923.60, 2854.18, and 1407.80 cm^{-1} on the scheelite surface, respectively. In addition, the skeleton vibration bands of N can be observed at 1614.15 and 1461.80 cm^{-1}, and the C–N band can be seen at 1349.95 cm^{-1}. These results indicate that ODB can also be adsorbed on the scheelite surface. However, given the amphoteric nature of ODB, the scheelite surface remains polar and hydrophilic. Consequently, it cannot float upward. After introducing 4wt% ODB into NaOl, the bands of $–CH_3$, $–CH_2–$ and –COOH could still be observed in the FTIR spectra of the scheelite surface. However, the bands of the nitrogen skeleton vibration of ODB do not appear. The results indicate that the adsorption of ODB on the scheelite surface is limited because of the low addition ratio, and the newly appearing bands mostly belong to NaOl. Therefore, the co-adsorption of ODB and NaOl on the scheelite surface is weak, and the synergistic effect of ODB is almost impossible by co-adsorption because ODB has no direct collection capacity.

3.3. XPS analysis results

As shown in Fig. 8(a), the synergistic mechanism of ODB is further illustrated by measuring the changes in the element types and chemical states on the scheelite surface after interaction with flotation reagents. The results of multiple scans reveal that the N content on the scheelite surface is lower than the detection limit of the instrument after the interaction with the combined collector (mass ratio of NaOl : ODB = 96:4), indicating that there is almost no adsorption of ODB on the scheelite surface, which is consistent with the results of FTIR spectral analysis.

Fig. 8(b) shows the Ca 2p spectra on scheelite under different collectors. Ca provides the adsorption sites for FAC and plays a crucial role in scheelite flotation [44–45]. Related studies have shown that Ca in scheelite crystals can be divided into fractured components (FC) and bulk components (BC) [46–47]. For bare scheelite, the binding energies of Ca $2p_{1/2}$ and $Ca2p_{3/2}$ in FC are 351.46 and 347.95 eV, respectively, and those of Ca $2p_{1/2}$ and Ca $2p_{3/2}$ in BC are 350.21 and 346.70 eV, respectively. Considering that the binding energy gap between Ca $2p_{1/2}$ and Ca $2p_{3/2}$ is fixed, Ca $2p_{1/2}$ was selected to investigate the relevant mechanism. After interaction with NaOl, the binding energies of Ca $2p_{1/2}$ in FC and BC on scheelite shifted by −0.23 and +0.10 eV, respectively. However, the binding energies of Ca in FC and BC on scheelite shifted by +0.84 and +0.34 eV after interaction with NaOl + ODB, respectively. These results suggest that ODB intensifies the chemical interaction between NaOl and Ca. The same variation pattern also appears for the binding energy of W 4f (Fig. 8(c)). The binding energies of W $4f_{5/2}$ and W $4f_{7/2}$ in bare scheelite are 37.29 and 35.19 eV, respectively. They are offset by +0.13 eV after acting with NaOl and +0.29 eV after acting with the combined reagent. As shown in Fig. 8(d), the peaks at 531.91 and 530.34 eV in the O 1s narrow spectra correspond to the binding energies of Ca–O and W–O, respectively [38,48–49]. After interaction with NaOl or the combined collector, new peaks at 532.92 or 533.38 eV can be attributed to O in –COOH of NaOl.

Consequently, it is difficult for ODB to have large-scale adsorption on the scheelite surface under the addition ratio of 4wt%. ODB may indirectly improve the collection capacity of NaOl at low temperatures by optimizing the foamability or

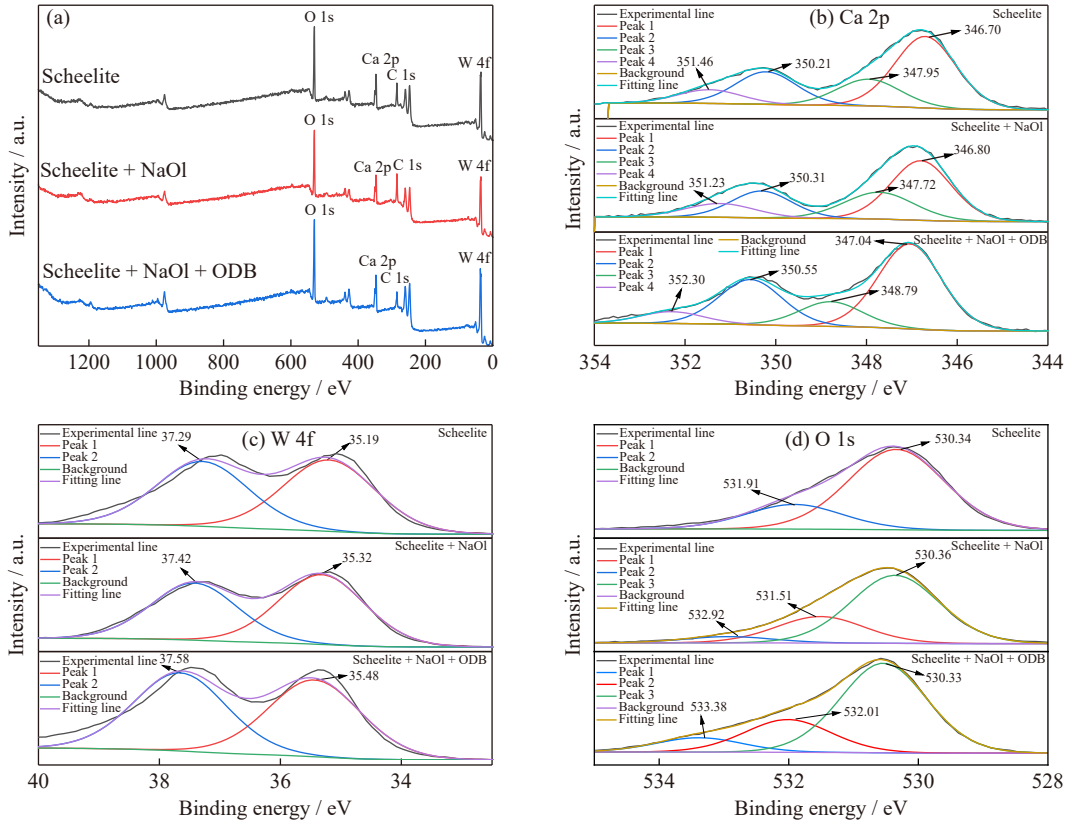

Fig. 8. XPS results of survey spectra and narrow spectra: (a) survey spectra; (b) Ca 2p; (c) W 4f; (d) O 1s.

dispersion.

3.4. Surface tension measurement results

As shown in Fig. 9(a), the CMCs of DDB, TDB, and ODB are 150, 100, and 30 mg/L, respectively, and the corresponding surface tension values are 16.9, 21.0, and 30.4 mN/m, respectively. The results indicate that the CMC of ADB decreases gradually with an increase in the length of the carbon chain because the mutual attraction among the hydrophobic groups of different molecules increases as the hydrocarbon chain of surfactants grows, which is more conducive to the formation of micelles [32,50]. Accordingly, ODB can effectively reduce the surface tension of the solution at a lower concentration, which corresponds to the results of the microflotation test. Fig. 9(b) illustrates that ODB reduces the CMC of NaOl solution from 300 to 100 mg/L at 10°C, indicating a synergistic effect between ODB and NaOl. Meanwhile, the surface tension of the combined collector is lower than that of NaOl at the same concentration before reaching CMC, which is more favorable to the foamability of NaOl.

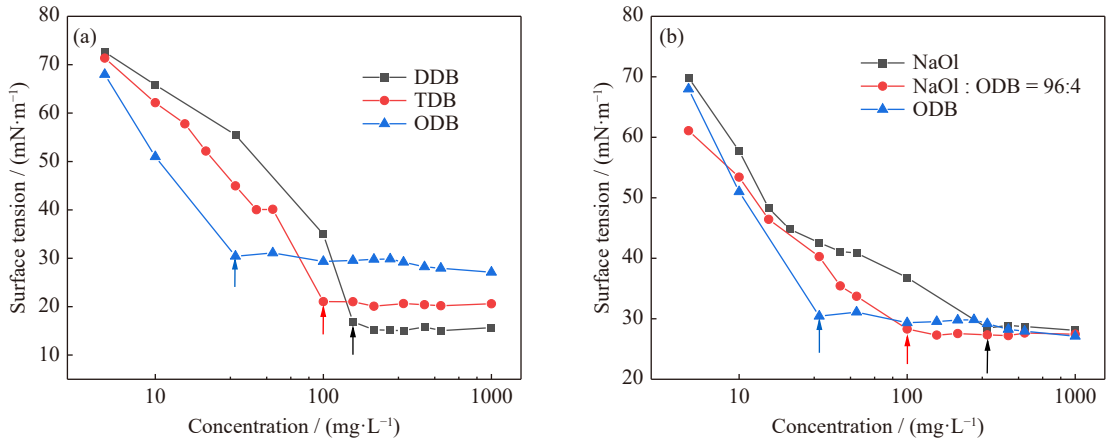

Fig. 9. Surface tension measurement results: (a) surface tension of ADB with different carbon chain lengths; (b) surface tension of the combined collector and individual components.

3.5. Foam performance testing and evaluation results

The effects of ODB on the foamability and foam stability of NaOl were evaluated at a low temperature (10°C). The collector concentration was fixed at 30 mg/L. As shown in Fig. 10, the foam volume increased with inflation time. The

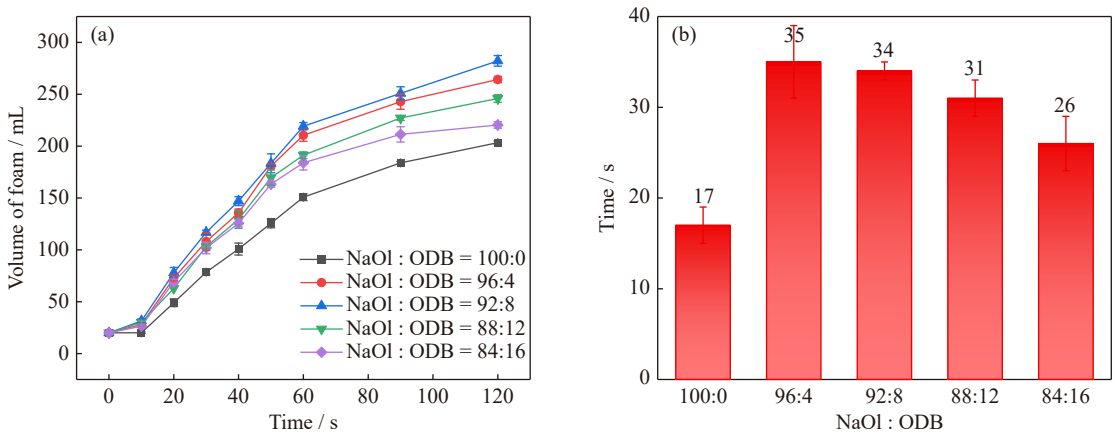

Fig. 10. Foam performance testing results: (a) effect of different ODB addition ratios on the foamability of the collector; (b) effect of different ODB addition ratios on the foam stability of the collector.

volume and the half-life of the foam of the combined collectors were greater than those of NaOl, which indicates that ODB improves the foamability and foam stability of NaOl at low temperatures. However, the foaming property and foam stability of NaOl will decline again when the ODB exceeds a certain ratio.

The analysis suggests that ODB and NaOl are co-distributed on the gas–liquid interface at the appropriate ratio. As ODB is an amphoteric surfactant with positive charges, it generates electrostatic attraction with the anions in NaOl, which weakens the electrostatic repulsion among the NaOl molecules. Consequently, the arrangement of surfactant molecules on the gas–liquid interface is compact. The mechanical strength of the foam increases, and air can hardly penetrate the liquid film of the foam, resulting in a lower probability of the foam bursting and a larger foam volume [26,51]. However, when the local liquid film is thinned because of foam collision, the excess ODB will cause the surfactant molecules to rapidly migrate to the surface of the liquid film, while the water molecules cannot be timely supplemented, and the liquid film remains thin, resulting in foam being mechanically weak [37,52–53]. Considering foamability and foam stability, the suitable ODB addition ratios are 4wt% and 8wt%. The results of flotation tests also indicated that NaOl has better collection capacity at these two ratios.

3.6. Flotation reagent size measurement results

The effect of ODB on the dispersion of NaOl was further investigated. As shown in Fig. 11, three reagents were dispersed in the solution in the form of aggregates. Apart from the intermolecular forces, electrostatic attractions were also observed among ODB molecules, which allow ODB to form larger agglomerates in an orderly arrangement. The same electrostatic attractions are also present between ODB and NaOl, resulting in the average distribution size of the combined reagent being slightly larger than that of NaOl alone. Given the deterioration of dispersion at low temperatures, the distribution size of NaOl, ODB, and their mixtures increased from 293.54 to 435.02, 1054.87 to 1186.77, and 341.14 to 353.65 nm, respectively, when the solution temperature was decreased from 25 to 10°C. The large cross-section of the

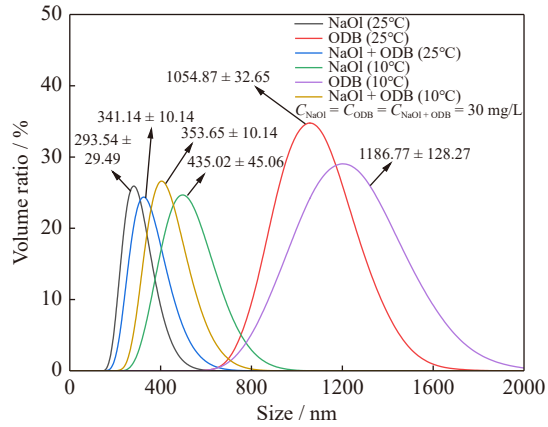

Fig. 11. Distribution size of different collectors in the same concentration (*C*) solution at different temperatures.

ammonium structure in ODB can improve the steric hindrance effect among the agglomerates in the combined collector and hinder the further increase of agglomerates in the combined collector at low temperatures. Meanwhile, the two polar groups in ODB can promote hydrophilicity of the agglomerates in the combined collector and boost the dispersibility of NaOl, which is equivalent to increasing the available concentration of NaOl. The synergistic mechanism of ODB for NaOl can be depicted in Fig. 12. ODB optimizes the foamability and dispersibility of NaOl at low temperatures.

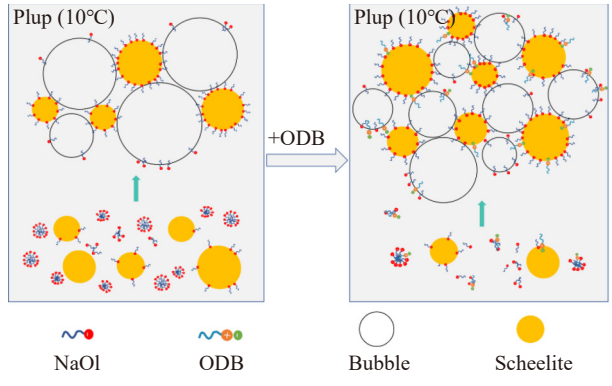

Fig. 12. Synergistic mechanism model of ODB for NaOl.

4. Conclusions

Betaine can activate the collection capacity of NaOl for scheelite at low temperatures, which enhances the recovery and utilization efficiency of scheelite and alleviates the production environment of the mining area. Based on the results of micro-flotation tests, the scheelite recovery increases from 85% to 91% with the addition ratio of ODB at 4%. ODB has the greatest effect on improving the collection capacity of NaOl at low temperatures among ADB with different chain lengths. The industrial test results indicate that the combined collector of ODB and NaOl is applied to the flotation of low-grade scheelite in the Luanchuan area, and the scheelite recovery can be increased by 3.48%. The combined collector has wide potential for application in scheelite plants in northern China.

The results of FTIR spectrum analysis, XPS analysis, surface tension measurement, foam performance testing, and dispersion size of the collector indicated that ODB does not have the collection capacity of scheelite, but it can improve the collection capacity of NaOl at low temperatures by optimizing the foaming characteristics and dispersion of NaOl. Furthermore, ODB can be used as a synergist alternative to improve the collection capacity of FAC in low-temperature environments.

Acknowledgements

This work was financially supported by the National Natural Science Foundation of China (Nos. 51904339 and No. 51974364), the Key Laboratory of Hunan Province for Clean and Efficient Utilization of Strategic Calcium-containing Mineral Resources, China (No. 2018TP1002), the Co-Innovation Centre for Clean and Efficient Utilization of Strategic Metal Mineral Resources, and the Postgraduate Independent Exploration and Innovation Project of Central South University, China (No. 2018zzts224).

Conflict of Interest

The authors declare no conflicts of interest.

Supplementary Information

The online version contains supplementary material at https://doi.org/10.1007/s12613-023-2718-2.

References

[1] Q.B. Cao, J.H. Cheng, S.M. Wen, C.X. Li, S.J. Bai, and D. Liu, A mixed collector system for phosphate flotation, *Miner. Eng.*, 78(2015), p. 114.

[2] F. Zhou, T. Chen, C.J. Yan, *et al*., The flotation of low-grade manganese ore using a novel linoleate hydroxamic acid, *Colloids Surf. A: Physicochem. Eng. Aspects*, 466(2015), p. 1.

[3] H.M. Yu, H.J. Wang, and C.Y. Sun, Comparative studies on phosphate ore flotation collectors prepared by hogwash oil from different regions, *Int. J. Min. Sci. Technol.*, 28(2018), No. 3, p. 453.

[4] X.M. Luo, W.Z. Yin, Y.F. Wang, C.Y. Sun, Y.Q. Ma, and J. Liu, Effect and mechanism of dolomite with different size fractions on hematite flotation using sodium oleate as collector, *J. Cent. South Univ.*, 23(2016), No. 3, p. 529.

[5] X. Wang, W.Q. Qin, F. Jiao, *et al*., Review of tungsten resource reserves, tungsten concentrate production and tungsten beneficiation technology in China, *Trans. Nonferrous Met. Soc. China*, 32(2022), No. 7, p. 2318.

[6] N. Kupka and M. Rudolph, Froth flotation of scheelite—A review, *Int. J. Min. Sci. Technol.*, 28(2018), No. 3, p. 373.

[7] W.H. Jia, W.Q. Qin, C. Chen, H.L. Zhu, and F. Jiao, Collecting performance of vegetable oils in scheelite flotation and differential analysis, *J. Cent. South Univ.*, 26(2019), No. 4, p. 787.

[8] W.D. Guo, Y.X. Han, Y.M. Zhu, Y.J. Li, and Z.D. Tang, Effect of amide group on the flotation performance of lauric acid, *Appl. Surf. Sci.*, 505(2020), art. No. 144627.

[9] H. Zhang, W.G. Liu, C. Han, and H.Q. Hao, Effects of monohydric alcohols on the flotation of magnesite and dolomite by sodium oleate, *J. Mol. Liq.*, 249(2018), p. 1060.

[10] J.F. He, C.G. Liu, and Y.K. Yao, Flotation intensification of the coal slime using a new compound collector and the interaction mechanism between the reagent and coal surface, *Powder Technol.*, 325(2018), p. 333.

[11] T. Coward, J.G.M. Lee, and G.S. Caldwell, Harvesting microalgae by CTAB-aided foam flotation increases lipid recovery and improves fatty acid methyl ester characteristics, *Biomass Bioenergy*, 67(2014), p. 354.

[12] M. Krasowska, J. Zawala, B.H. Bradshaw-Hajek, J.K. Ferri, and D.A. Beattie, Interfacial characterisation for flotation: 1. solid-liquid interface, *Curr. Opin. Colloid Interface Sci.*, 37(2018), p. 61.

[13] A. Vidyadhar, N. Kumari, and R.P. Bhagat, Adsorption mechanism of mixed collector systems on hematite flotation, *Miner. Eng.*, 26(2012), p. 102.

[14] J. Tian, L.H. Xu, W. Deng, H. Jiang, Z.Y. Gao, and Y.H. Hu, Adsorption mechanism of new mixed anionic/cationic collectors in a spodumene-feldspar flotation system, *Chem. Eng. Sci.*, 164(2017), p. 99.

[15] D. López-Díaz, I. García-Mateos, and M.M. Velázquez, Synergism in mixtures of zwitterionic and ionic surfactants, *Colloids Surf. A: Physicochem. Eng. Aspects*, 270-271(2005), p. 153.

[16] W.H. Jia, F. Jiao, H.L. Zhu, L. Xu, and W.Q. Qin, Mitigating the negative effects of feldspar slime on spodumene flotation using mixed anionic/cationic collector, *Miner. Eng.*, 168(2021), art. No. 106813.

[17] L.O. Filippov, I.V. Filippova, Z. Lafhaj, and D. Fornasiero, The role of a fatty alcohol in improving calcium minerals flotation with oleate, *Colloids Surf. A: Physicochem. Eng. Aspects*, 560(2019), p. 410.

[18] H. Sis and S. Chander, Improving froth characteristics and flotation recovery of phosphate ores with nonionic surfactants, *Miner. Eng.*, 16(2003), No. 7, p. 587.

[19] K. Theander and R.J. Pugh, Synergism and foaming properties in mixed nonionic/fatty acid soap surfactant systems, *J. Colloid Interface Sci.*, 267(2003), No. 1, p. 9.

[20] C. Chen, H.L. Zhu, W. Sun, Y.H. Hu, W.Q. Qin, and R.Q. Liu, Synergetic effect of the mixed anionic/non-ionic collectors in low temperature flotation of scheelite, *Minerals*, 7(2017), No. 6, art. No. 87.

[21] W.H. Sun, W.G. Liu, S.J. Dai, T. Yang, H. Duan, and W.B. Liu, Effect of Tween 80 on flotation separation of magnesite and dolomite using NaOL as the collector, *J. Mol. Liq.*, 315(2020), art. No. 113712.

[22] Z.Y. Liu, Z.C. Xu, H. Zhou, *et al*., Interfacial behaviors of betaine and binary betaine/carboxylic acid mixtures in molecular

dynamics simulation, *J. Mol. Liq.*, 240(2017), p. 412.
[23] J.B. Yang and J.R. Hou, Synthesis of erucic amide propyl betaine compound fracturing fluid system, *Colloids Surf. A: Physicochem. Eng. Aspects*, 602(2020), art. No. 125098.
[24] X.L. Lu, M. Zhang, L. Xie, and Q. Zhou, Coagulative colloidal gas aphrons generated from polyaluminum chloride (PACl)/dodecyl dimethyl betaine (BS-12) solution: Interfacial characteristics and flotation potential, *Colloids Surf. A: Physicochem. Eng. Aspects*, 530(2017), p. 209.
[25] Z.H. Zhou, D.S. Ma, Q. Zhang, *et al*., Surface dilational rheology of betaine surfactants: Effect of molecular structures, *Colloids Surf. A: Physicochem. Eng. Aspects*, 538(2018), p. 739.
[26] W.Y. Shao, J.Y. Zhang, K. Wang, C.R. Liu, and S.M. Cui, Cocamidopropyl betaine-assisted foam separation of freshwater microalgae *Desmodesmus brasiliensis*, *Biochem. Eng. J.*, 140(2018), p. 38.
[27] X. Wang, W.Q. Qin, F. Jiao, *et al*., Review on development of low-grade scheelite recovery from molybdenum tailings in Luanchuan, China: A case study of Luoyang Yulu Mining Company, *Trans. Nonferrous Met. Soc. China*, 32(2022), No. 3, p. 980.
[28] X. Wang, W.H. Jia, C.R. Yang, *et al*., Innovative application of sodium tripolyphosphate for the flotation separation of scheelite from calcite, *Miner. Eng.*, 170(2021), art. No. 106981.
[29] N. Kupka and M. Rudolph, Role of sodium carbonate in scheelite flotation—A multi-faceted reagent, *Miner. Eng.*, 129(2018), p. 120.
[30] Y. Foucaud, L. Filippov, I. Filippova, and M. Badawi, The challenge of tungsten skarn processing by froth flotation: A review, *Front. Chem.*, 8(2020), art. No. 230.
[31] X. Wang, H. Song, F. Jiao, *et al*., Utilization of wastewater from zeolite production in synthesis of flotation reagents, *Trans. Nonferrous Met. Soc. China*, 30(2020), No. 11, p. 3093.
[32] T. Gaudin, P. Rotureau, I. Pezron, and G. Fayet, Investigating the impact of sugar-based surfactants structure on surface tension at critical micelle concentration with structure-property relationships, *J. Colloid Interface Sci.*, 516(2018), p. 162.
[33] E. Calvo, R. Bravo, A. Amigo, and J. Gracia-Fadrique, Dynamic surface tension, critical micelle concentration, and activity coefficients of aqueous solutions of nonyl phenol ethoxylates, *Fluid Phase Equilib.*, 282(2009), No. 1, p. 14.
[34] J. Church, M.R. Willner, B.R. Renfro, *et al*., Impact of interfacial tension and critical micelle concentration on bilgewater oil separation, *J. Water Process. Eng.*, 39(2021), art. No. 101684.
[35] A. Pal, R. Punia, and G.P. Dubey, Formation of mixed micelles in an aqueous mixture of a biamphiphilic surface active ionic liquid and an anionic surfactant: Experimental and theoretical study, *J. Mol. Liq.*, 337(2021), art. No. 116355.
[36] S.M.S. Hussain, M.S. Kamal, and L.T. Fogang, Synthesis and physicochemical investigation of betaine type polyoxyethylene zwitterionic surfactants containing different ionic headgroups, *J. Mol. Struct.*, 1178(2019), p. 83.
[37] A. Atrafi and M. Pawlik, Foamability of fatty acid solutions and surfactant transfer between foam and solution phases, *Miner. Eng.*, 100(2017), p. 99.
[38] Y.F. Cui, F. Jiao, Q. Wei, X. Wang, and L.Y. Dong, Flotation separation of fluorite from calcite using sulfonated lignite as depressant, *Sep. Purif. Technol.*, 242(2020), art. No. 116698.
[39] X. Wang, F. Jiao, W.Q. Qin, *et al*., Sulfonated brown coal: A novel depressant for the selective flotation of scheelite from calcite, *Colloids Surf. A: Physicochem. Eng. Aspects*, 602(2020), art. No. 125006.
[40] Q.Y. Meng, Q.M. Feng, and L.M. Ou, Flotation behavior and adsorption mechanism of fine wolframite with octyl hydroxamic acid, *J. Cent. South Univ.*, 23(2016), No. 6, p. 1339.
[41] G. Güler, R.M. Gärtner, C. Ziegler, and W. Mäntele, Lipid-protein interactions in the regulated betaine symporter BetP probed by infrared spectroscopy, *J. Biol. Chem.*, 291(2016), No. 9, p. 4295.
[42] C. Harbeck, R. Faurie, and T. Scheper, Application of near-infrared spectroscopy in the sugar industry for the detection of betaine, *Anal. Chim. Acta*, 501(2004), No. 2, p. 249.
[43] H. Kumar, J. Kaur, and P. Awasthi, Scrutinizing the micellization behaviour of 14-2-14 gemini surfactant and tetradecyltrimethylammonium bromide in aqueous solutions of betaine hydrochloride drug, *J. Mol. Liq.*, 338(2021), art. No. 116642.
[44] C.H. Zhang, Y.H. Hu, W. Sun, J.H. Zhai, Z.G. Yin, and Q.J. Guan, Effect of phytic acid on the surface properties of scheelite and fluorite for their selective flotation, *Colloids Surf. A: Physicochem. Eng. Aspects*, 573(2019), p. 80.
[45] W.P. Yan, C. Liu, G.H. Ai, Q.M. Feng, and W.C. Zhang, Flotation separation of scheelite from calcite using mixed collectors, *Int. J. Miner. Process.*, 169(2017), p. 106.
[46] C. Wang, S. Ren, W. Sun, *et al*., Selective flotation of scheelite from calcite using a novel self-assembled collector, *Miner. Eng.*, 171(2021), art. No. 107120.
[47] Z.Y. Gao, Z.Y. Jiang, W. Sun, *et al*., New role of the conventional foamer sodium N-lauroylsarcosinate as a selective collector for the separation of calcium minerals, *J. Mol. Liq.*, 318(2020), art. No. 114031.
[48] F. Jiao, L.Y. Dong, W.Q. Qin, W. Liu, and C.Q. Hu, Flotation separation of scheelite from calcite using pectin as depressant, *Miner. Eng.*, 136(2019), p. 120.
[49] Q. Wei, L.Y. Dong, F. Jiao, and W.Q. Qin, Selective flotation separation of fluorite from calcite by using sesbania gum as depressant, *Miner. Eng.*, 174(2021), art. No. 107239.
[50] S.F. Burlatsky, V.V. Atrazhev, D.V. Dmitriev, *et al*., Surface tension model for surfactant solutions at the critical micelle concentration, *J. Colloid Interface Sci.*, 393(2013), p. 151.
[51] Q. Lin, K.H. Liu, Z.G. Cui, X.M. Pei, J.Z. Jiang, and B.L. Song, pH-Responsive Pickering foams stabilized by silica nanoparticles in combination with trace amount of dodecyl dimethyl carboxyl betaine, *Colloids Surf. A: Physicochem. Eng. Aspects*, 544(2018), p. 44.
[52] A. Atrafi, C.O. Gomez, J.A. Finch, and M. Pawlik, Frothing behavior of aqueous solutions of oleic acid, *Miner. Eng.*, 36-38(2012), p. 138.
[53] C. Da, S. Alzobaidi, G.Q. Jian, *et al*., Carbon dioxide/water foams stabilized with a zwitterionic surfactant at temperatures up to 150°C in high salinity brine, *J. Petrol. Sci. Eng.*, 166(2018), p. 880.